Chemical Engineering Journal 103 (2004) 77–88

Chemical Engineering Journal

www.elsevier.com/locate/cej

Evaluation of a monolith reactor for the catalytic wet oxidation of cellulose

Benjamin D. Schutt, Martin A. Abraham*

Department of Chemical and Environmental Engineering, The University of Toledo, 2801 W. Bancroft St., Toledo, OH 43606, USA

Received 3 October 2003; accepted 19 May 2004

Abstract

The catalytic wet air oxidation of cellulose, a model compound for biomass, was evaluated in a monolith froth reactor to assess its application for the conversion of biomass-containing aqueous streams. Both the conversion of cellulose and the formation of more highly oxidized products increased with the presence of a palladium catalyst when compared with a blank monolith. A comparison between the monolith froth reactor and a batch reactor was completed, demonstrating for the first time the mass transfer benefits of this novel reactor to more conventional reactor systems.

The effects of base additives on cellulose degradation were also investigated. Reactions were performed in a pH range from 7 to 11.5 and indicated that the reaction rates increased with an increase in the pH of the feed solution. However, relatively little change in reaction rate was observed when the cation of the base was varied. A lumped (three parameter) kinetics analysis based on first order kinetics, consistent with oxidation of similar systems reported in literature, was used to evaluate the performance of the reactor under various feed conditions.

Keywords: Monolith reactor; Catalytic wet oxidation; Cellulose

1. Introduction

Biomass is defined as “non-fossil . . . forms of carbon and includes all land and water-based vegetation . . . that have intrinsic chemical energy content” [1]. Recent trends in developing renewable resources has refocused efforts to utilize biomass as a feedstock in producing fuels and chemicals. Often, conversion concepts are built from the idea of the “biomass refinery”, in which solid biomass is first decomposed into basic chemical feedstocks and then rearranged into desired chemical products [2]. An abundant supply of biomass resources can be found in certain waste streams, such as wood and wood wastes, agricultural crops and their waste by-products, municipal solid waste (MSW), industrial wastes (e.g. paper pulping mill waste), animal manure, forestry residuals, waste from food processing, and dead biomass that results from nature’s life cycles.

The use of biomass as a renewable feedstock for the production of fuels and specialty chemicals is a work in progress. Kuznetsov [3] states that renewable wood biomass can successfully produce all common “petrochemical” products plus unique organic compounds. However, this technology is not economically competitive with the production of fuels and specialty chemicals from fossil resources. The degradation and oxidation of cellulose into carboxylic acids is an important step towards developing a process for the use of biomass as a viable feedstock.

Approximately 40–50% of woody biomass is cellulose [3], a natural biopolymer that is highly cross-linked and very stable. As a major component of most biomass, knowledge about the conversion of cellulose is important for processes which use biomass as a feedstock and for those in which biomass must be decomposed within a waste treatment process. While biomass is highly available, the stability of the cellulose structure, largely due to the presence of covalent bonds, hydrogen bonds [4], and van der Waals forces [5], makes selective conversion difficult.

* Corresponding author. Tel.: +1 419 530 8092; fax: +1 419 530 8086.
E-mail address: martin.abraham@utoledo.edu (M.A. Abraham).

1385-8947/$ – see front matter © 2004 Elsevier B.V. All rights reserved.
doi:10.1016/j.cej.2004.05.016

Non-selective decomposition of biomass can be accomplished through chemical or biological means [6], and is well-known. For example, direct hydrolysis of cellulosic materials to liquids has been known for more than 100 years [1], and results in the formation of D-glucose units, and other depolymerization products. Enhancement through pH adjustment has been reported using dilute acid [7] or through base catalysis with NaOH [4,8,9]. Recent results on the base-catalyzed conversion of glucose in supercritical water, and its comparison with cellulose conversion, reveal the large number of products that can be formed and the benefits of modeling cellulose reactions with glucose [10].

Other thermal processes for cellulose conversion include wet air oxidation (WAO), a well-established technique for the treatment of wastewater streams containing organic or toxic constituents [11]. WAO is defined as the oxidation of organic and inorganic substances in an aqueous solution or suspension by means of reaction with oxygen (usually air) at elevated temperatures of 125–315 °C and pressures of 0.5–15 MPa. Operating at elevated temperatures and pressures enhances the solubility of oxygen and provides a strong driving force for oxidation. Through this process, insoluble organic matter is converted to low molecular weight compounds consisting primarily of carboxylic acids and other carbonyl-group compounds. If reaction conditions are severe enough, carbon dioxide and water will be produced as end products.

In order to enhance the oxidation rate, catalysts may be used during WAO processes. For example, Abbadi and van Bekkum [12] reported that elevated pH could be used to enhance the Pt-catalyzed oxidation of D-glucose. Working with a 5% Pt/C catalyst, they determined an optimum pH of 9, controlled throughout the run with KOH, for glucose oxidation, with decreasing performance as the pH was decreased. For homogeneous liquids, the use of a solid catalyst to enhance wet oxidation results in a three-phase process; if insoluble cellulose was to be used as the feedstock, a four-phase process would result.

Multiphase reactions are conventionally carried out in slurry and trickle bed reactors, in which mass transfer and fluid flow parameters are optimized to provide maximum performance [13]. As an alternative, we have evaluated the use of a monolith to support heterogeneous catalysts during oxidation in compressed water. Monoliths consist of uniform, parallel, non-connecting capillary channels that have a honeycomb structure. The main advantages of these supports are low-pressure drop, high external area to volume ratio, excellent mechanical strength, uniform flow characteristics through the monolith channels, and flow of fluids containing particulates. The reactor is designed to provide two-phase bubble train flow, consisting of a steady stream of alternating gas bubbles and liquid slugs that move upwards through the monolith channel, as defined by Thulasidas et al. [14], within the channels of the monolith.

In a previous study [15], catalytic WAO of acetic acid was achieved with a Pt/Al_2O_3 catalyst supported on a monolith. The two-phase flow or froth was fed from the bottom of the monolith channels and the reaction occurred at the monolith surface. The monolith froth reactor has also been demonstrated for the catalytic oxidation of glucose and cellulose [16]. Catalytic enhancement was observed for glucose oxidation with a platinum catalyst supported on the monolith; however, the oxidation rate of cellulose was slow due to it being insoluble in aqueous media.

Within the current paper, we report on the advantage obtained from combining a monolith-supported catalyst with modification of solution pH for the conversion of cellulose in aqueous media. By combining the preferential cellulose hydrolysis achieved through the addition of basic species with the catalytic oxidation promoted by palladium metal, we demonstrate the opportunity for process intensification in the conversion of cellulose particulate matter in aqueous media. Several base additives were evaluated in the monolith reactor and compared with uncatalyzed conversion and operation in a more conventional batch reactor system.

2. Experimental

Most experiments were completed in the monolith froth reactor shown in Fig. 1, which is described briefly below and in more detail elsewhere [15]. Comparative experiments were performed in a contained-solids stirred semi-batch reactor, shown in Fig. 2.

2.1. Monolith froth reactor

The monolith froth reactor (MFR) contains four sections: liquid and gas feed, reactor, and separator. The liquid feed consists of a recycle tank, high-pressure liquid pump, and flush tank; the liquid feed lines were wrapped with heating tape (Omega model STH51-060). The gas feed consists of a gas cylinder, heating system and mass flow meter (Omega model FMA-871-V); the gas then passed through 0.635 cm stainless steel tubing where it was heated with a 1.27 cm × 1.83 m heating tape (Omega model STH51-060) that was wrapped around the tubing and insulated with fiberglass insulation tape. The heating load was controlled by a PID controller (LFE model 1400). The reactor system includes a frothing section, monolith catalyst, tubular reactor, heating system and thermocouples, and pressure transducer (Omega model PX612-3KGV). The separation system includes a gas–liquid separator, cooling tank, thermocouple, and visual level gauge to ensure liquid–vapor phase separation. Product gas was directed to an on-line gas chromatograph for regular analysis (see Section 2.3 further). The liquid was directed to the recycle tank, from which samples were periodically withdrawn for off-line analysis by gas chromatography. To ensure safe working conditions, 1/2 in. thick Plexiglas sheets were attached to the experimental structure and surrounded all high-pressure components of the experimen-

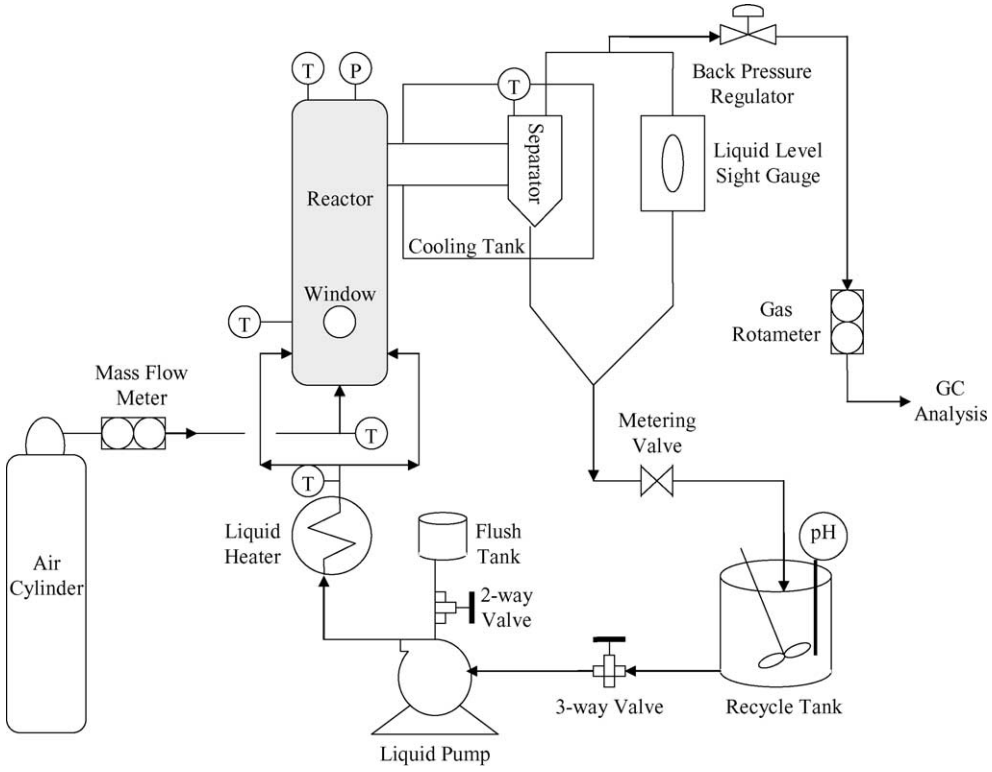

Fig. 1. Schematic diagram of the experimental system.

tal system. The reactor system has been described in more detail previously [17].

The liquid feed to the reactor was modified by the incorporation of a flush tank that was connected in-line with the pump. The flush tank was used to back flush the pump and clear any cellulose that may have begun to clog it. The flush tank consisted of a 530 cm^3 acrylic cylindrical tank connected to the pump through 4 mm i.d. plastic tubing and a two-way ball valve (Hoke model 7115-F4Y). The back flush liquid was collected by means of a three-way ball valve (Whitey

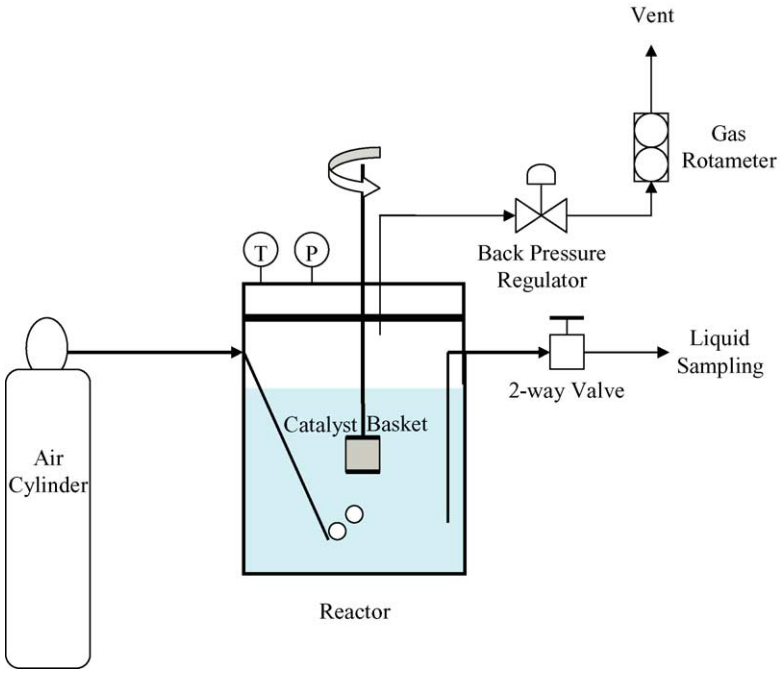

Fig. 2. Schematic diagram of batch reactor system used for comparison with the monolith reactor.

model 45XS8) placed between the recycle tank and the pump.

Catalyst was prepared using the incipient wetness technique described previously [16]. The monolith cores were cut from 62 cell/cm^2 Honeyceram monolith bricks, that had been previously coated with a γ-Al_2O_3 washcoat. The cores were cut to the desired specifications, 4.3 cm in diameter and 10.9 cm in length, using a 4.7 cm i.d. core bit and a drill press. The cores were impregnated with a solution of palladium acetylacetonate (Strem Chemical) in toluene, containing 1.58 g palladium. During the impregnation, the monolith cores were repeatedly dipped into this solution and dried under nitrogen at 50 °C between loadings. Once the loading process was complete, the impregnated cores were calcined in an oven at 250 °C for 6 h. After all of the experiments were complete, Schwarzkopf Microanalytical Laboratory analyzed the used catalyst for Pd content. A 0.64 wt.% was found on the catalyst, indicating 1.41 g Pd on the monolith supports and suggesting essentially no loss of palladium throughout the course of the experiments.

2.2. Batch reactor system

A batch experimental system, shown schematically in Fig. 2, was developed from an Autoclave Engineers stirred reactor and had an operating range up to 37.2 MPa at 343 °C. The reactor was equipped with a rupture disc (Autoclave Engineers) rated to 34.4 MPa. The heating source for the batch reactor was a clamp-on ceramic heating jacket (Industrial Heater Corporation). A PID controller (LFE model 1410), which supplied power to the heating jacket based on the temperature in the reactor, controlled the heating load. The conditions inside the reactor were monitored with a thermocouple (Type K) and a pressure transducer (Sensotech). To ensure safe working conditions, 1/2 in. thick Plexiglas shields were placed between the operator and the experimental equipment. These shields were removed only when sampling occurred.

The reactor was equipped with a 0.159-cm 316 stainless steel tube that fed gas to the bottom of the reactor and was positioned so that the gas would bubble up through the catalyst located in a stainless steel mesh (Spectrum Labs) basket attached to the spinning shaft. The gas was fed to the reactor via this tubing from a high-pressure air cylinder through a compressed gas regulator (Victor model SR 4J) and rose out of the top of the reactor through a backpressure regulator (GO model BP-60), which controlled the reactor pressure. The gas then flowed through a rotameter (Gilmont model 13) where the effluent gas flow rate was measured. The gas was then released to a laboratory fume hood.

The batch reactor was charged with 0.2 g cellulose and 200 mL of deionized water giving a concentration of 1000 ppm. A fresh portion of the monolith catalyst prepared for the MFR was crushed to about 100 μm and placed in the mesh baskets in the reactor. The reactor was then sealed, after which the gas flow was started. The reactor pressure was slowly increased while maintaining a constant gas flow rate. Once the desired pressure was achieved, the temperature controller was set. After the temperature achieved a stable value, the stirrer was activated and the stopwatch time was noted as the zero time for the reaction. This startup procedure took approximately 25 min for each of the batch experiments.

Liquid samples were taken through 0.159 cm stainless steel tube inserted in the reactor. Liquid was pushed through this sampling tube by the force of pressure. The resultant liquid flow rate was throttled with a two-way straight valve (HiP). Due to the experimental setup, the pH of the feed solution could not be continuously adjusted, so the pH was measured at the beginning and the end of the experimental run. The final pH for the Pd coated and blank support experiments were 8.7 and 9.0, respectively. This change in pH was due to the formation of acidic products during the reaction. There were also limitations in obtaining an accurate sample of the cellulose concentration from the batch reactor during an experimental run; thus, only the cellulose conversion at the end of the batch experiments was recorded.

2.3. Analytical information

The cellulose used in all experiments was pure microcrystalline cellulose powder (CAS no. 9004-34-6), with a particle size of approximately 20 μm, purchased from Aldrich Chemical Company, Inc. (Product no. 310697) and used as received. The cellulose was added to a volume of deionized water so that a concentration of 1000 ppm(w) was attained.

The amount of cellulose in the solution was determined through two different measurements. Solid cellulose was measured by filtration. Liquid samples were collected and filtered under vacuum through pre-weighed 0.2 μm pore size Millipore filters and rinsed once with 10 mL of deionized water. The filters were then dried in vacuum at 50 °C and reweighed once they had cooled. A similar method was used in a previous study to measure insoluble cellulose [9].

Soluble liquid products were quantified on a Shimadzu high performance liquid chromatography (HPLC) equipped with a photodiode array detector measuring at a wavelength of 210 nm. The separation of the reaction products was achieved by Sugar Series SH 1011 packed column (Shodex). Elution was performed at 0.65 mL/min flow rate of mobile phase (0.005 M H_2SO_4) and a column temperature of 35 °C. The concentration of cellulosic oligomer was evaluated by decomposing the cellulose using cellulase enzyme (Sigma Chemical) and glucose (HK) reagent (Sigma Diagnostics) and then completing a liquid phase analysis.

Gas samples from the MFR were analyzed online using an Hewlett Packard 5890A gas chromatograph (GC) equipped with a thermal conductivity detector. The gas products were separated using an 80/100 mesh Porapak N 0.635 cm × 304.8 cm stainless steel column with an oven temperature of 50 °C and helium as the carrier gas. The detector temperature was 120 °C. The GC was calibrated for CO_2 prior to all experiments.

3. Results and discussion

The oxidation of cellulose was evaluated as a function of added base by (1) varying the cation and (2) increasing the hydroxide ion concentration (pH) with the use of the same cation. All efforts were made to duplicate the same experimental conditions (temperature, pressure, and liquid and gas flow rates) for each experiment. The liquid flow rate for all data sets was 30 mL/min and the gas flow rate was 2.53 SLPM. An initial cellulose concentration of 1000 ppm was used. The temperature of the reactor was set at 130 °C, an appropriate reaction temperature determined in previous experiments [15], and the reactor pressure for each experiment was maintained at 1.93 MPa, above the vapor pressure of water at the operating temperature.

During the experimental runs, cellulose was degraded and subsequently oxidized into products. HPLC analysis was used for the qualitative and quantitative determination of the products formed, which were identified as cellulosic oligomer and glucose along with oxalic, malic, succinic, and acetic acids. These products were recorded as a function of time throughout a 6 h experimental run.

Fig. 3a shows the yield of the major products (glucose, succinic acid, and acetic acid) and the conversion of the solid cellulose as a function of time for an experiment at pH 9 (controlled with $Na_2B_4O_7$). In addition, Fig. 3b shows the yield of the minor products (oxalic acid, malic acid, and cellulosic oligomer) formed during the same experiment as a function of time. The formation of these species through partial oxidation of cellulose is consistent with results previously reported for the monolith reactor [16]. In both figures, the points represent the experimental data while the curves for product yields and cellulose conversion were drawn using best-fit second order polynomials to better visualize the trends in the data. Yield is defined on the basis of initial solid cellulose that could be converted to products (described as amorphous cellulose) and was thus determined as:

$$\text{yield} = \frac{\text{mass of product}}{\text{initial mass of reactive cellulose}} \quad (1)$$

Similarly, the conversion was based on the initial mass of reactive cellulose:

$$\text{conversion} = 1 - \frac{\text{mass of remaining cellulose}}{\text{initial mass of reactive cellulose}} \quad (2)$$

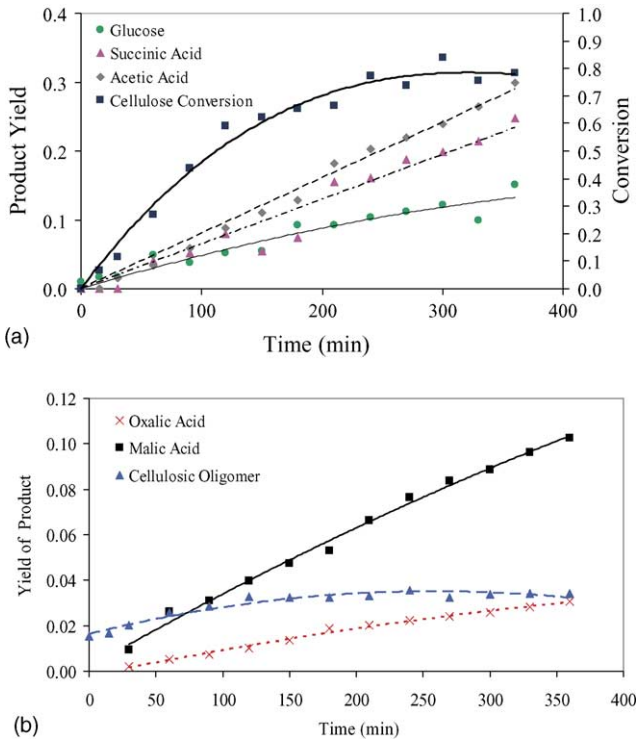

Fig. 3. Reaction product profile from experiment 23, a typical experiment controlled to pH = 10 using $Na_2B_4O_7$. (a) Cellulose conversion and yield of major products. (b) Yield of minor products.

Even though high cellulose reactivity was observed, the maximum conversion that was achieved in any of the experiments was 40%, on a weight basis. It is well known that cellulose is composed of both crystalline and amorphous domains [18]. Since the crystalline domain is generally resistant to oxidation, we assumed that the amorphous domain of the cellulose was the only portion available for reaction, and comprised 40% of the original sample. Thus, yield and conversion was calculated by assuming that the initial mass of reactive cellulose was 40% of the initial cellulose charge.

A carbon balance was determined as the total amount of cellulose converted during the course of the experiment and the measured amount of cellulosic oligomer, glucose and carboxylic acids formed during each experiment. The percent of carbon contributed by these products and the residual cellulose remaining after a 6 h experiment was divided by the percent of carbon in the initial charge of cellulose. For all experiments in this study, the average carbon balance was 0.90 (±0.2). Additional carbon mass could have been produced through the formation of CO_2 or other volatile organic compounds (VOC's) that may have passed through the GC undetected. The carbon dioxide detection limit was determined to be 1.46×10^{-8} moles (based on our sample loop volume of 0.5 mL), which could have produced 9.42×10^{-3} moles of CO_2 over the course of a 6 h experiment. If this amount of carbon dioxide had been formed, then the average carbon balance would have been 0.95 (±0.2). The inclusion of other VOC's that may have been present in the gas phase would lead to a carbon balance closer to 1.

The remaining portion of the unaccounted carbon could have been in the form of undetected liquid products. Although many of the liquid products were identified and quantified through HPLC analysis, not all of the peaks in the HPLC analysis were positively identified. Numerous attempts were made to match small unidentified peaks to the peak retention times of various known compounds, however, the identity of these liquid products could not be determined. In a study of D-glucose oxidation with a platinum catalyst, Abbadi and van Bekkum [12] reported the main products formed

were D-gluconic acid, 2-keto-D-gluconic acid, L-guluronic acid, D-glucaric acid, and D-arabinoic acid. Other components that have been identified during cellulose degradation include furfural and hydroxymethyl-furfural [19]. Since cellulose is made up of D-glucose units linked by glycosidic bonds, it is likely that these acids comprise the bulk of the unidentified minor species.

3.1. Kinetic analysis

Cellulose is a chain of D-glucose units linked by glycosidic bonds. During the degradation of cellulose, these chains are broken to form products with a lower degree of polymerization, such as cellulosic oligomers or individual glucose units. It has been reported through previous studies that these cellulose derived products can be further degraded and oxidized into carboxylic acids [11,12,16,20]. However, the exact mechanism of cellulose degradation and oxidation is very complex because the reaction pathways lead to the formation of multiple intermediates.

Six different species were identified as products of cellulose degradation during the course of this study. Previous literature has modeled such complicated processes by lumping the products formed [21,22]. By employing this same technique, a three parameter mathematical model was developed to represent the current results. A lumped parameter model provides a basis for engineering analysis of the results, without requiring detailed mechanistic information that can not be obtain based on the current experimental effort.

The lumped kinetic model is indicated in Fig. 4, where the cellulose component is represented by *A*, cellulosic oligomer and glucose products (soluble sugars) are lumped as a single pseudo-component *B*, and the carboxylic acid products are lumped as pseudo-component *C*. Cellulosic oligomer and glucose products were lumped as one component because these compounds are formed as an intermediate from cellulose before being further oxidized into carboxylic acids. The carboxylic acids represent another lump in the model because these compounds are more highly degraded products of cellulose and are generally stable at the reaction conditions used here. Some carboxylic acids, such as acetic acid, are very resistant to further degradation and are generally considered an end product in most reaction processes.

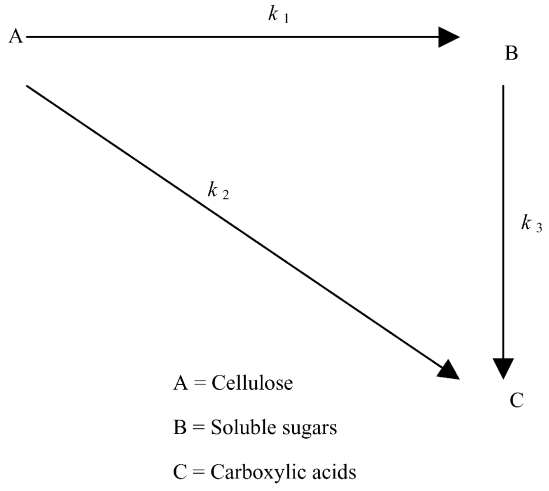

Fig. 4. Proposed lumped reaction pathways used to model reaction performance.

It was previously reported [16] that a reaction pathway involving cellulose degradation into cellulosic oligomers and glucose products was thermally enhanced and these intermediates were then oxidized into carboxylic acids through a metal catalyst enhancement ($A \rightarrow B \rightarrow C$). The current model combines the catalytic pathway with a direct pathway for the conversion of cellulose into carboxylic acids ($A \rightarrow$ C). This additional pathway may be base-catalyzed, in accord with base addition in the current experiments. Basic solutions induce swelling in the cellulose, which makes its structure more vulnerable to degradation. With increased reactivity, it may have been possible to convert the cellulose directly to a carboxylic acid.

First-order kinetic behavior was assumed for each of the reaction pathways. Considerable investigations on WAO of different types of organic compounds have revealed that first-order kinetics provides a reasonable model in most cases [23]. Studies on CWAO of bleach plant effluents have also suggested first-order kinetics [21]. In addition, an attempt was made to model the data with half-order, first-order and second-order kinetics, and the first-order kinetic behavior was found to give the best representation of the data collected. Thus, the rate equations for the lumped parameter system were written as

$$-r_A = -\frac{dA}{dt} = (k_1 + k_2)A \tag{3}$$

$$r_B = \frac{dB}{dt} = k_1 A - k_3 B \tag{4}$$

$$r_C = \frac{dC}{dt} = k_2 A + k_3 B \tag{5}$$

These rate equations were used to solve for the predicted pseudo-components *A*, *B* and *C* as a function of time for each experiment. The reaction rate constants (k_1, k_2, and k_3) were selected to minimize the sum of squares (SSQ) difference between the predicted lumped components and their measured values:

$$SSQ = \sum[(A_i - \hat{A}_i)^2 + (B_i - \hat{B}_i)^2 + (C_i - \hat{C}_i)^2] \tag{6}$$

using the Microsoft Excel Solver function. Once the sum of squares error was minimized, the reaction rate constants for a specific experiment could be recorded. The result of this kinetic modeling is shown in Fig. 5 for a typical experiment performed at a pH 10. The points represent the experimental data from experiment 14 (NaOH, pH = 10), while the lines represent the model prediction. Although the experimental data does not exactly duplicate the curves of the mathematically predicted model, it does match the general trends.

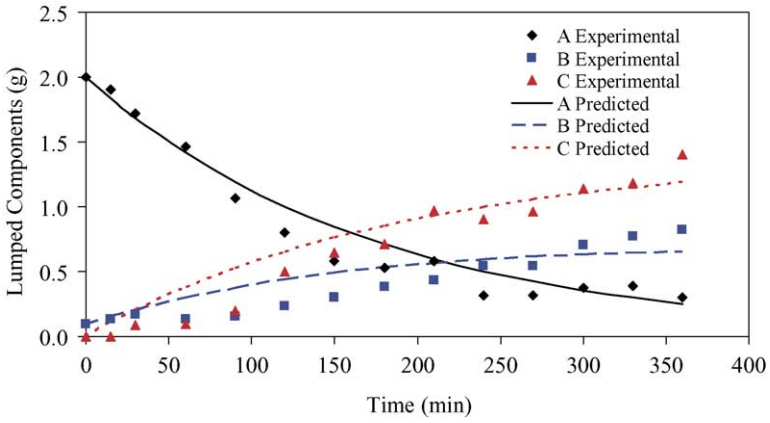

Fig. 5. Comparison of experimental data with predications of the lumped kinetic model, for experiment 14 controlled to pH = 10 using NaOH.

Table 1 is a summary of the results from the sum of squares analysis for all of the experimental runs. This table includes each of the experiments conducted in this study and the basic species that were used to control the pH of the feed solution. The reaction rate constants are those values determined to minimize the error between the model prediction and the experimental measurements, and the sample variance (σ) was calculated for each experiment,

$$\sigma = \frac{\sum \left[(A_i - \hat{A}_i)^2 + (B_i - \hat{B}_i)^2 + (C_i - \hat{C}_i)^2 \right]}{n} \quad (7)$$

where n is the number of measurements. A small variance indicates a high quality of fit between the model predictions and the experimental data. The results provided in Table 1 reveal generally good agreement of the model with the experimental data.

3.2. Effect of hydroxide ion concentration

The effect of hydroxide ion concentration, [OH^-], on reactor performance was evaluated at three pH values (7, 10, and 11.5) using NaOH. In these experiments, the pH of the feed solution was continuously monitored and controlled throughout the reaction with the addition of 7.5 M NaOH solution, prepared by dissolving the requisite amount of solute in deionized water. The concentration of this solution was arbitrarily chosen.

The effect of hydroxide ion concentration, [OH^-], on reactor performance is indicated in Fig. 6a as a plot of cellulose conversion versus reaction run time, parametric in solution pH. The points in Fig. 6a represent the experimental data while the lines represent the model fit using the rate constants of Table 1. Cellulose conversion increased with an increase in pH of the liquid feed solution.

Fig. 6b compares the final yield of major products as a function of solution pH, and reveals that higher pH resulted in a larger yield of products. At pH 10 and 11.5 comparable yields of glucose were formed, but nearly twice as much acetic acid, a highly oxidized product, was produced at pH 11.5. This figure illustrates that conversion of cellulose into carboxylic acids can be enhanced by controlling the pH.

The effect of increased [OH^-] is also illustrated by the increasing values of the rate constants k_1 and k_2 at higher pH, as

Table 1
Kinetic results from the sum of squares analysis

Experiment	Conditions	k_1 (min^{-1})	k_2 (min^{-1})	k_3 (min^{-1})	Sample variance
12	No controls pH: 4	9.531E-04	8.672E-04	7.098E-04	0.0551
13	NaOH pH: 7	1.733E-03	1.589E-03	8.030E-04	0.0997
14	NaOH pH: 10	2.050E-03	3.696E-03	3.672E-04	0.0195
15	$Ca(OH)_2$ pH: 7	2.315E-03	1.381E-03	1.202E-03	0.1254
16	$Ca(OH)_2$ pH: 9.2	1.612E-03	2.068E-03	1.232E-04	0.1404
17	NaOH pH: 11.5	3.524E-03	7.613E-03	3.785E-03	0.0588
18	KOH pH: 10	2.367E-03	2.797E-03	4.799E-04	0.0968
19	KOH pH: 7	1.445E-03	1.395E-03	6.314E-04	0.0712
20	$Ba(OH)_2$ pH: 9.2	1.538E-03	1.647E-03	2.655E-04	0.1697
21	$Na_2B_4O_7$ pH: 9.0	2.235E-03	2.466E-03	4.153E-03	0.0168
22[a]	NaOH pH: 10	1.031E-03	1.253E-04	0.000E+00	0.0050
23[a]	$Na_2B_4O_7$ pH: 9.0	4.493E-04	4.450E-04	0.000E+00	0.0169
24[b]	NaOH pH: 10	3.417E-04	1.201E-04	2.248E-03	0.0015
25[ab]	NaOH pH: 10	1.290E-04	1.423E-04	0.000E+00	0.0003

[a] Blank monolith.
[b] Batch reactions.

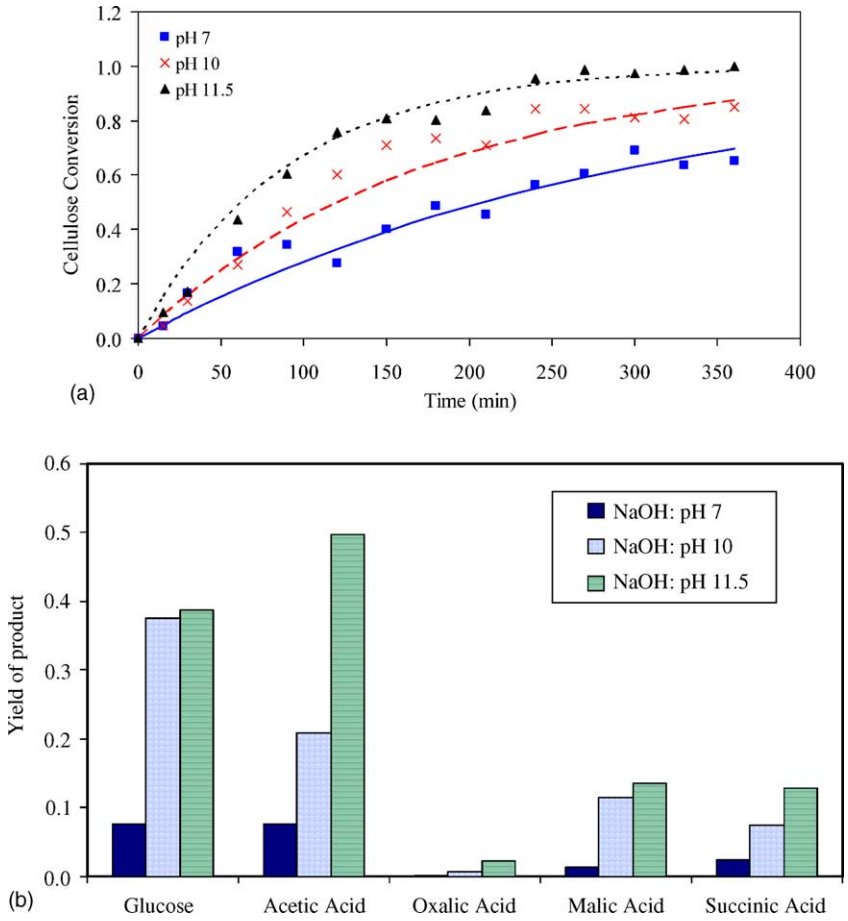

Fig. 6. The effect of solution pH on the performance of the monolith reactor. (a) Conversion of cellulose and comparison with model predictions. (b) Final yield of major products.

indicated in Table 1. This result is consistent with previous results in which higher cellulose conversion was the result of changes in the cellulose structure caused by its exposure to OH^-. Structural change of cellulose through exposure to aqueous solutions of NaOH has been observed by other studies [4,9], which found through X-ray diffraction that there was an apparent decrease in the crystalline pattern from the initial cellulose pulp to the insoluble residue after treatment with NaOH. Tahiri and Vignon [20] report that the degradation process is hampered by the crystallinity of the cellulose and the poor accessibility of the primary hydroxyl groups, which are partly engaged in hydrogen bonding between surface species.

3.3. *Effects of different bases*

The effect of using different bases to control the pH is indicated in Fig. 7 as a bar graph of the reaction rate constants for each base at approximately equivalent pH. Experiments were conducted using five different bases; $Ca(OH)_2$, $Ba(OH)_2$, KOH, NaOH, and $Na_2B_4O_7$ and their controlled pH values were 9.2, 9.2, 10, 10 and 9, respectively. $Ca(OH)_2$ and $Ba(OH)_2$ were chosen to represent hydroxides of the alkaline earths (group 2A), KOH and NaOH were chosen to represent the hydroxides of the alkali metals (group 1A), and $Na_2B_4O_7$ was chosen as a Lewis base for comparison against the four Bronsted–Lowry bases. An attempt was made to control all of the experiments to pH 10, but due to a combination of the experimental equipment and the solubility limit of

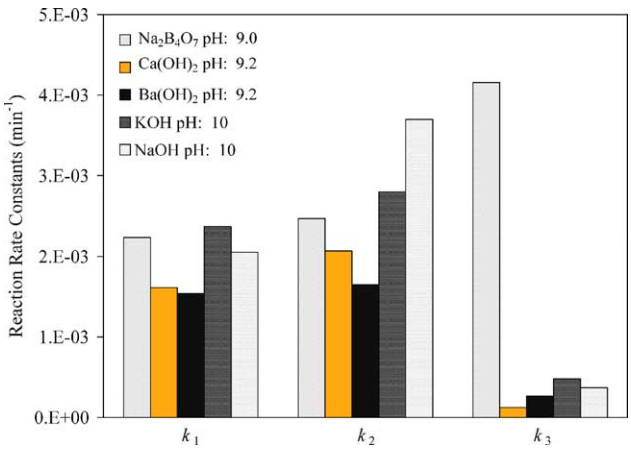

Fig. 7. The role of cation on the calculated values of rate constants obtained from the kinetic model describing the conversion of cellulose.

some of the bases, this level could not be achieved for all of the experiments.

Fig. 7 indicates that the conversion of cellulose into cellulosic oligomers and glucose (k_1) or directly into carboxylic acids (k_2) is mostly independent of the type of base used. While the best-fit values for k_2 were higher for NaOH and KOH than the other bases, the pH used in these experiments were also slightly higher. As determined previously, an increase in pH should lead to a higher value of k_2. This also indicates that [OH^-] had a greater effect on cellulose conversion then the specific cation associated with the base.

Fig. 7 also indicates that the k_3 value for the experimental run controlled with $Na_2B_4O_7$ was much higher than the k_3 values of the other bases. k_3 is the rate constant for the reaction path where cellulosic oligomer and glucose products are converted into carboxylic acids. Previous research [16] reported that the rate of this reaction pathway was enhanced by the presence of a metal catalyst. It would seem that this base, $Na_2B_4O_7$, assisted the metal catalyst with the conversion of the intermediate cellulosic oligomers and glucose into carboxylic acids. This may have been the result of greater interactions between the Lewis base and the intermediates relative to that of the Bronsted–Lowry bases. Further investigation into the effects of this base would be required in order to demonstrate this result in a consistent pattern.

3.4. Demonstration of the catalytic effect of palladium

The performance of the palladium coated monolith catalyst was compared against a "blank" monolith, which is a monolith with no metal catalyst, in the MFR. Two reaction conditions were evaluated for each monolith; NaOH (pH 10) and $Na_2B_4O_7$ (pH 9) and an average reactor temperature of 135 and 129 °C, respectively. The performance of the Pd coated and blank monoliths were evaluated by their ability to degrade and oxidize cellulose.

The monoliths' ability to degrade the cellulose is indicated in Fig. 8a as a plot of cellulose conversion versus reaction run time for the four experiments. The points in Fig. 8a represent the experimental data while the curves represent the model fit using the rate constants of Table 1. The conversion of the cellulose with the blank monolith was approximately one-third of that of the Pd coated monolith in both basic solutions.

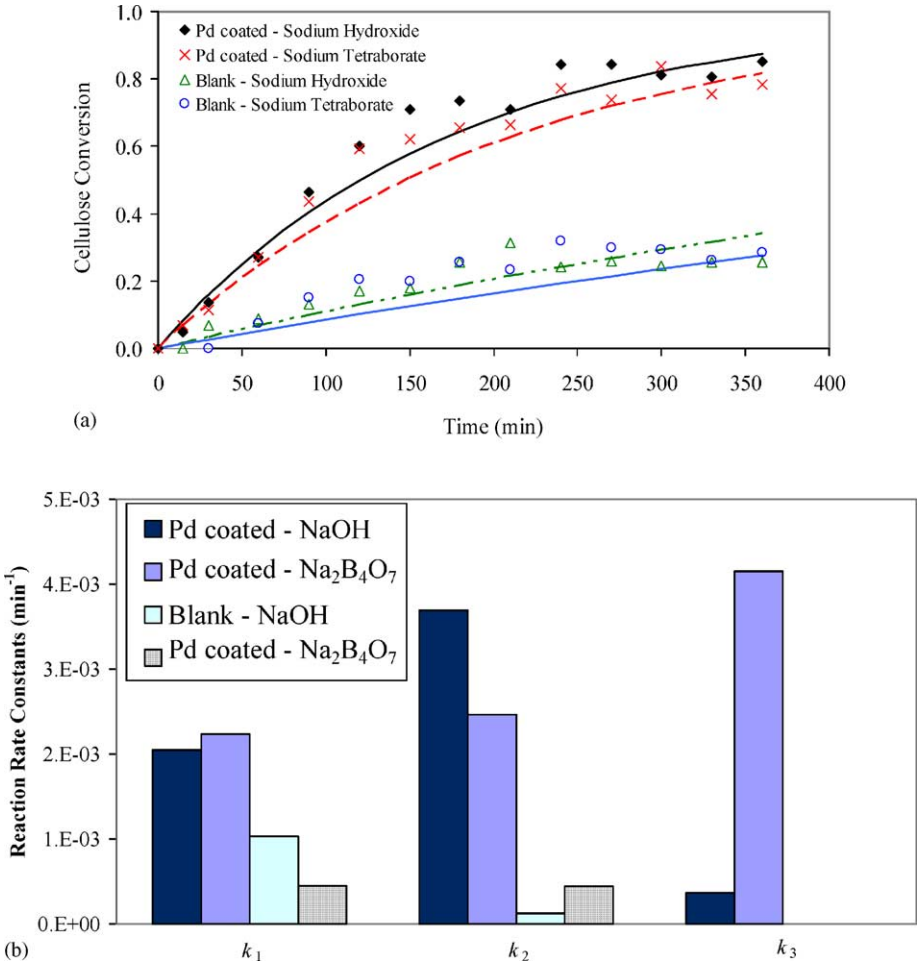

Fig. 8. Comparison of palladium-catalyzed oxidation of cellulose with performance of an uncoated monolith. (a) Cellulose conversion and model predictions and (b) final yield of major products.

Clearly, the palladium on the monolith acted as a catalyst that enhanced the overall rate of cellulose degradation.

The palladium coated monolith also gave much greater yields of both acetic acid and glucose in comparison to the blank monoliths in the presence of both bases. Glucose and acetic acid were the only products detected from the blank monolith, while the Pd coated monolith also produced oxalic, malic and succinic acids. This illustrates the importance of the metal catalyst for the production of carboxylic acids. The presence of the palladium catalyst accelerated both the rate of cellulose decomposition and the amount of products formed after a given reaction time.

The reaction rate constants calculated from the lumped parameter model also demonstrate the reaction enhancement obtained from the Pd coated monolith relative to the blank, as shown in Fig. 8b. The rate constant k_1 determined for the blank monoliths was approximately one-third of the values recorded for the Pd coated monolith and the k_2 values for the blank monoliths were approximately 1/10 of the values for the Pd coated monolith. The much higher value of k_1 for the Pd coated monolith relative to the blank monolith indicates that the metal catalyst enhanced the reaction pathway of cellulose degradation into cellulosic oligomer and glucose products. The higher value for k_2 also indicates that the Pd catalyst had an effect on the direct conversion of cellulose into carboxylic acids. However, it is clear that the heterogeneous catalyst was effective in accelerating the conversion of cellulose.

It is also important to note that the k_3 values for the blank monoliths were found to be zero, confirming previous reports that the dissolved species in the liquid phase (i.e. cellulosic oligomers and glucose) followed a metal catalyzed pathway to the formation of carboxylic acids [16]. In the absence of the palladium catalyst, this reaction pathway was not available to promote the degradation and oxidation of cellulose into carboxylic acids.

3.5. Monolith froth reactor versus batch reactor

A comparison between the performance of the monolith froth reactor and a batch reactor was based on the conversion of cellulose after a 6 h experimental run. Four experiments were considered in this comparison. All effort was made to create the same conditions (reactor temperature and pressure, gas flow rate, ratio of support to feed solution) for each experiment.

Two experiments were conducted in both the monolith froth reactor and the batch reactor; one with a Pd coated monolith and the other with a blank monolith. These experiments were run at a pH 10 with NaOH and an initial cellulose concentration of 1000 ppm. The pH of the feed solution in the monolith reactor experiment was continuously monitored and controlled throughout the reaction whereas the pH of the solution in the batch reactor varied with reaction time.

Fig. 9a compares both the conversion of cellulose and the yields of glucose and acetic acid from the MFR with that of the batch reactor and indicates that the MFR gave substantially higher cellulose conversion relative to the batch reactor for both the Pd coated and blank support experiments. There was nearly a six-fold enhancement in cellulose conversion with the Pd coated monolith and nearly a three-fold enhancement with the blank monolith in comparison to the batch reactor results. The cellulose conversion from the MFR experiment with a Pd coated monolith controlled to pH 7 with NaOH was still substantially higher than the comparable batch experiment and demonstrates that the enhanced performance of the MFR was not simply due to the higher pH that was maintained throughout the run. The batch reactor with the Pd catalyst produced only small amounts of glucose and acetic acid, while the monolith froth reactor with the Pd catalyst produced larger amounts of glucose and acetic acid as well as malic, succinic and oxalic acids. The batch reactor with the blank produced more glucose and acetic acid than the monolith froth reactor with the blank, in contrast to the result observed when palladium catalyst was utilized.

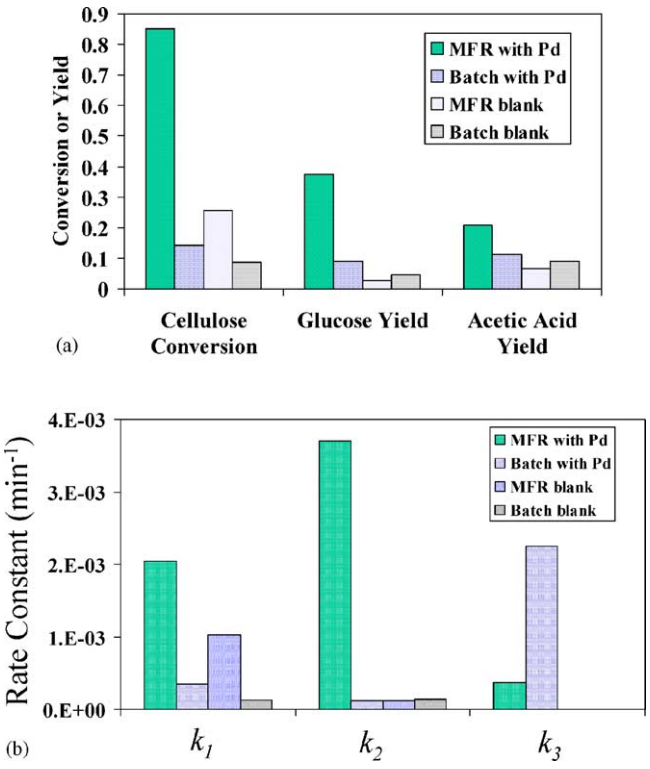

Fig. 9. Comparison of the performance of the monolith froth reactor with a batch reactor operating under similar reaction conditions. (a) Cellulose conversion after 6 h. (b) Final yield of major products.

Analysis of the rate constants reported in Table 1 and shown in Fig. 9b reveals that the k_1 values from the batch reactor were approximately one-sixth of that for the monolith froth reactor. The k_2 value for the MFR with the Pd coated monolith showed a 30-fold enhancement over the Pd coated support in the batch reactor. However, the batch reactor with the Pd coated support showed a six-fold enhancement in k_3

over the MFR with the Pd coated monolith. The k_3 values were found to be zero for the blank supports.

Assuming equivalent gas–liquid mass transfer parameters, the batch reactor and the MFR should give equivalent results. However, the MFR was substantially more successful in converting cellulose than the batch reactor. The increase in k_1 values for the MFR shows that it had an advantage in degrading the cellulose into cellulosic oligomer and glucose products. The increased k_2 value for the MFR with Pd coated catalyst shows the advantage offered through the monolith catalyst. According to the previous analysis of the MFR [14], two-phase flow within the channels of the monolith provided a higher rate of mass transfer for oxygen through the liquid phase to the surface of the catalyst, thereby enhancing cellulose conversion directly into carboxylic acid. In the batch reactor, this pathway was not favored, and intermediate cellulosic oligomer and glucose products were produced and converted into carboxylic acids.

The results of these experiments show that the monolith froth reactor performed better than the batch reactor for the degradation and oxidation of solid cellulose. It is suggested that this advantage is a result of the unique flow patterns found in the MFR, which leads to minimal mass transfer resistance between the gas and solid phase. The batch reactor did not provide good contact of the phases in the reactor, leading to the relatively poor performance that is observed. While it is possible that better performance could have been obtained in the batch reactor by modifying the gas distribution system or increasing the stirrer speed, the current data suggests an advantage for the use of a monolith froth reactor for biomass oxidation.

4. Conclusions

The degradation and oxidation of cellulose over a palladium monolith catalyst was chosen as a model reaction to evaluate the performance of a monolith froth reactor for its possible application in the conversion of biomass-containing aqueous streams. A three-parameter mathematical model was developed and successfully applied to fit the experimental data. This model was used to estimate rate constants, which were used for comparing the effects of palladium catalyst, pH, base additives, and reactor systems. The palladium catalyst provided a three-fold enhancement in cellulose conversion when compared against a blank. Greater formation of carboxylic acids was also noted with the catalyst. This was a surprising impact of the palladium heterogeneous catalyst since cellulose is generally insoluble in aqueous media.

Increasing the pH of the feed solution increased the rate of cellulose oxidation in the presence of the Pd catalyst. Variance in the cation of the base additives did not have a substantial effect on the oxidation of cellulose. However, $Na_2B_4O_7$, a Lewis base, appeared to catalyze the conversion of soluble sugars to carboxylic acids, based on the value of the rate constant for this pathway in the kinetic model.

The monolith froth reactor was found to hold an advantage over the batch reactor for the oxidation of cellulose. Higher cellulose conversion and a greater yield of partial oxidation products were produced by the monolith froth reactor particularly when palladium catalyst was used. The advantage of the monolith froth reactor was attributed to a high catalyst surface area available on the monolith, good fluid mixing as previously observed for two-phase in monoliths [14], and low mass transfer resistance through a very thin liquid film to the surface of the catalyst.

References

[1] D.L. Klass, Biomass for Renewable Energy, Fuels, and Chemicals, Academic Press, San Diego, 1998.
[2] S. Varadarajan, D.J. Miller, Catalytic upgrading of fermentation-derived organic acids, Biotechnol. Prog. 15 (5) (1999) 845–854.
[3] B.N. Kuznetsov, Application of catalysts for producing organic compounds from plant biomass, React. Kinet. Catal. Lett. 57 (1996) 217–225.
[4] L. Rahkamo, L. Viikari, J. Buchert, T. Paakkari, T. Suortti, Enzymatic and alkaline treatments of hardwood dissolving pulp, Cellulose 5 (1998) 79–88.
[5] A.C. O'Sullivan, Cellulose: the structure slowly unravels, Cellulose 4 (3) (1997) 173–207.
[6] E. Varga, A.S. Schmidt, K. Reczey, A.B. Thomsen, Pretreatment of corn stover using wet oxidation to enhance enzymatic digestibility, Appl. Biochem. Biotechnol. 104 (1) (2003) 37–50.
[7] F. Camacho, P. Gonzalez-Tello, E. Jurado, A. Robles, Microcryalline-cellulose hydrolysis with concentrated sulphuric acid, J. Chem. Tech. Biotechnol. 67 (1996) 350–356.
[8] A.M. Shaker, Base-catalyzed oxidation carboxymethyl-cellulose polymer by permanganate, J. Colloid Interface Sci. 233 (2001) 197–204.
[9] A. Isogai, R.H. Atalla, Dissolution of cellulose in aqueous NaOH solutions, Cellulose 5 (1998) 309–319.
[10] A. Sinag, A. Kruse, V. Schwarzkopf, Key compounds of the hydropyrolysis of glucose in supercritical water in the presence of K_2CO_3, Ind. Eng. Chem. Res. 42 (15) (2003) 3516–3521.
[11] F. Luck, A review of industrial catalytic wet air oxidation processes, Catal. Today 27 (1996) 195–202.
[12] A. Abbadi, H. van Bekkum, Effect of pH in the Pt-catalyzed oxidation of D-glucose to D-gluconic Acid, J. Mol. Catal. A Chem. 97 (1995) 111–118.
[13] G.F. Froment, K.B. Bischoff, Chemical Reactor Analysis and Design, second ed., Wiley, New York, 1990.
[14] T.C. Thulasidas, M.A. Abraham, R.L. Cerro, Bubble-train flow in capillaries of circular and square cross section, Chem. Eng. Sci. 50 (1995) 183.
[15] A.A. Klinghoffer, R.L. Cerro, M.A. Abraham, Influence of flow properties on the performance of the monolith froth reactor for catalytic wet oxidation of acetic acid, Ind. Eng. Chem. Res. 37 (4) (1998) 1203–1210.
[16] T.A. Patrick, M.A. Abraham, Evaluation of a monolith-supported Pt/Al_2O_3 catalyst for wet oxidation of carbohydrate-containing waste streams, Environ. Sci. Technol. 34 (2000) 3480–3488.
[17] B.D. Schutt, B. Serrano, R.L. Cerro, M.A. Abraham, Production of chemicals from cellulose and biomass-derived compounds through catalytic sub-critical water oxidation in a monolith reactor, Biomass Bioenergy 22 (2002) 365–375.
[18] A.M. Emsley, R.J. Heywood, M. Ali, C.M. Eley, On the kinetics of degradation of cellulose, Cellulose 4 (1997) 1–5.

[19] A.B. Bjerre, A.B. Olesen, T. Fernquist, A. Ploger, A.S. Schmidt, Pretreatment of wheat straw using combined wet oxidation and alkaline hydrolysis resulting in convertible cellulose and hemicellulose, Biotech. Bioeng. 49 (1996) 568–577.
[20] C. Tahiri, M.R. Vignon, TEMPO-oxidation of cellulose: synthesis and characterization of polyglucuronas, Cellulose 7 (2000) 177–188.
[21] L.X. Li, P.S. Chen, E.F. Gloyna, Generalized kinetic model for wet oxidation of organic compounds, AIChE J 37 (11) (1991) 1687–1697.
[22] Q. Zhang, K.T. Chuang, Lumped kinetic model for CWO of organic compounds in industrial wastewater, AIChE J. 45 (1999) 145–150.
[23] V.S. Mishra, V.V. Mahajani, J.B. Joshi, Wet air oxidation, Ind. Eng. Chem. Res. 34 (1995).